Progress In Electromagnetics Research Letters, Vol. 95, 25–32, 2021

Augmented Quaternion MUSIC Method for a Uniform/Sparse COLD Array

Zhiwei Jiang[1], Zehao Zhang[1], Tianyi Zhao[1], Hua Chen[1, 2, *], and Weifeng Wang[3]

Abstract—The quaternion multiple signal classification (Q-MUSIC) algorithm reduces the dimension of covariance matrix, which would result in performance degrading of DOA estimation. An augmented quaternion MUSIC algorithm (AQ-MUSIC) based on concentered orthogonal loop and dipole (COLD) array is presented in this paper. The proposed algorithm uses an augmented quaternion formalism to model the completely polarized signals, which allows a concise and novel way to an augmented covariance matrix. The fact reveals that more accurate DOA parameters could be extracted from an augmented covariance matrix. Even compared with the long vector MUSIC (LV-MUSIC) algorithm whose dimension of covariance matrix is the same as AQ-MUSIC, the accuracy of DOA parameter estimation is also improved. Simulation results verify the performance promotion of the proposed approach.

1. INTRODUCTION

Compared with the conventional scalar array, the electromagnetic vector sensor array is a superior array, which contains not only the incident sources' spatial information, but also the polarization information. As such it has many applications in radar, sonar, wireless communications, etc. [1–4]. A large number of works have been conducted by extending the classical scalar array processing techniques to the vector-sensor case, such as MUSIC-like [5, 6] and ESPRIT-like [7, 8] methods dealing with multi-components of vector sensor array with different configurations. The vector sensor array considered in the above mentioned methods is formulated in the real or complex field, as arranged one by one into a "long-vector". Although "long-vector" subspace-based approaches appear to have a better performance than classical scalar ones, they have the drawback of ignoring possible structural information of the vector-type signal.

Further, by maintaining the vector nature of array output, some efforts have been devoted to vector array signal processing in quaternion framework. Those works demonstrated the advantages of vector sensor array in DOA estimation accuracy and robustness to model errors. For instance, MUSIC-like DOA estimators were formed for vector-sensor arrays, based on quaternion [9], biquaternion [10], and quad-quaternion [11] data models, respectively, achieving equivalent or superior performance to their complex counterparts as a result of utilizing strict orthogonality. Besides, despite less memory required for data covariance representation in quaternion or biquaternion framework, the dimension of corresponding data covariance is also reduced, which may result in a degraded performance because the DOA estimation accuracy of the MUSIC-like methods mainly depends on the dimension of the noise subspace of the covariance matrix.

Received 23 October 2020, Accepted 5 December 2020, Scheduled 9 December 2020
* Corresponding author: Hua Chen (dkchenhua0714@hotmail.com).
[1] Faculty of Electrical Engineering and Computer Science, Ningbo University, Ningbo 315211, China. [2] Key Laboratory of Intelligent Perception and Advanced Control of State Ethnic Affairs Commission, Dalian 116600, China. [3] The 54th Research Institute of China Electronics Technology Group Corporation (CETC54), Shijiazhuang 050081, China.

In this paper, we propose an augmented quaternion MUSIC (AQ-MUSIC) algorithm based on a concentered orthogonal loop and dipole (COLD) uniform linear array (ULA)/sparse linear array (SLA) by concatenating two quaternion models. Based on the AQ model, the AQ noise subspace is obtained by performing eigenvalue decomposition (EVD) of the adjoint matrix of AQ covariance matrix calculated with the AQ observations. Then the interesting DOAs are estimated based on the AQ-MUSIC estimators by distinguishing the peaks. The superior performance of the proposed algorithm is shown through computer simulations, as compared with the existing MUSIC-like counterparts. Therefore, the proposed method can be better effectively applied in wireless monitoring applications than existing methods by resorting to a more efficient patch antenna [12].

Notations: $(\cdot)^*$, $(\cdot)^T$, and $(\cdot)^H$ denote conjugate, transpose, and conjugate transpose, respectively; $\text{diag}\{\cdot\}$ and $\text{blkdiag}[\cdot,\cdot]$ denote the diagonal and block diagonal matrices, respectively; $\mathbf{I}_k$ denotes the k-dimensional identity matrix; $E(\cdot)$ and $det(\cdot)$ are the expectation and determinant operators, respectively. $\|\cdot\|_F^2$ denotes the Frobenius norm. $\mathbb{R}$, $\mathbb{C}$, and $\mathbb{H}$ represent real, complex, and quaternion fields, respectively.

2. QUATERNIONS AND POLARIZATION MODEL

2.1. Quaternions

A quaternion q has four components with one real part and three imaginary parts, which can be represented in Cayley-Dickson form as [9–11]:

$$\begin{aligned} q &= r_0 + r_1 i + r_2 j + r_3 k \\ &= c_1 + c_2 j, \end{aligned} \tag{1}$$

where $r_0, r_1, r_2, r_3 \in \mathbb{R}$ are real numbers; $c_1 = r_0 + r_1 i, c_2 = r_2 + r_3 i \in \mathbb{C}$ are complex numbers; and i, j, k are three imaginary units obeying the following rules:

$$\begin{aligned} &ij = -ji = k, \qquad jk = -kj = i, \\ &ki = -ik = j, \qquad i^2 = j^2 = k^2 = -1. \end{aligned} \tag{2}$$

Then, we introduce an important theorem of quaternion matrix used in our proposed algorithm. Given a square quaternion matrix $\mathbf{B} \in \mathbb{H}^{M\times M}$, the eigenvalue decomposition of its adjoint matrix $\mathbf{B}^\sigma$ can be expressed as [4]:

$$\mathbf{B}^\sigma = \begin{bmatrix} \mathbf{U}_1 & \mathbf{U}_2 \\ -\mathbf{U}_2^* & \mathbf{U}_1^* \end{bmatrix} \begin{bmatrix} \mathbf{D} & \mathbf{0} \\ \mathbf{0} & \mathbf{D}^* \end{bmatrix} \begin{bmatrix} \mathbf{U}_1 & \mathbf{U}_2 \\ -\mathbf{U}_2^* & \mathbf{U}_1^* \end{bmatrix}^H = \mathbf{U}_c \mathbf{D}_c \mathbf{U}_c^H. \tag{3}$$

In Eq. (3), the eigenvalues of $\mathbf{B}^\sigma$ appear in conjugated pairs, contributing to diagonal matrices $\mathbf{D} \in \mathbb{H}^{M\times M}$ and $\mathbf{D}^* \in \mathbb{H}^{M\times M}$, and $\mathbf{D}_c$ and $\mathbf{U}_c$ are the adjoint matrices of $\mathbf{D}$ and $\mathbf{U} = \mathbf{U}_1 + \mathbf{U}_2 j$, respectively. Therefore, the eigenvalue decomposition of the quaternion matrix $\mathbf{B}$ is given by

$$\mathbf{B} = (\mathbf{U}_1 + \mathbf{U}_2 j)\mathbf{D}(\mathbf{U}_1 + \mathbf{U}_2 j)^H. \tag{4}$$

In particular, when $\mathbf{B}$ is a Hermitian matrix, $\mathbf{D}$ is a real diagonal matrix.

2.2. Polarization Model

Consider a ULA consisting of M pairs of COLD, which are located on y-axis with the center at $y = md$ $(m = 1, \dots, M)$, as shown in Fig. 1 of [7]. The distance d between two adjacent COLD pairs is assumed within a half-wavelength to avoid angle ambiguity. Assume that K far-field completely polarized signals $s_k(t), k = 1, \dots, K$ impinge on the array from $\theta_k, k = 1, \dots, K$ in the y-z plane, where θ_k denotes the angle of the kth source measured from the z-axis, and the steering vector $\mathbf{a}(\theta_k)$ is the response of the array corresponding to the kth DOA. With respect to the element at the origin of the axes, the mth element of $\mathbf{a}(\theta_k)$ is defined as $a_m(\theta_k)=e^{im\gamma_k}$, where $\gamma_k = -\frac{2\pi d}{\lambda}\sin\theta_k$, and λ is the wavelength of the signal.

The response of a COLD can be decomposed into electric field components and magnetic field components. The loop and dipole arranged respectively in the x-direction and z-direction measure each component separately, with the dipole measuring the electric component and the loop measuring the magnetic component. Hence, for the kth signal, the components of the signal received by a COLD can be defined as [7]

$$\begin{aligned}\boldsymbol{\xi}_k &= \begin{bmatrix} \xi_{k,1} \\ \xi_{k,2} \end{bmatrix} \\ &= \begin{bmatrix} -\sin\varphi_k & \cos\theta_k\cos\varphi_k \\ -\cos\theta_k\cos\varphi_k & -\sin\varphi_k \end{bmatrix} \begin{bmatrix} \cos\alpha_k \\ \sin\alpha_k e^{i\beta_k} \end{bmatrix}\end{aligned} \tag{5}$$

where $0 \leq \alpha_k \leq \pi/2$ and $0 \leq \beta_k \leq 2\pi$ are the ranges of the polarization angle and phase difference, respectively, while φ_k is the angle of the kth source measured from the x-axis, as we assume that all sources are in the y-z plane, which means $\varphi_k = 90°$. Therefore $\boldsymbol{\xi}_k$ can be simplified as

$$\boldsymbol{\xi}_k = \begin{bmatrix} -1 & 0 \\ 0 & -1 \end{bmatrix} \begin{bmatrix} \cos\alpha_k \\ \sin\alpha_k e^{i\beta_k} \end{bmatrix}. \tag{6}$$

Thus, the signal vector $\mathbf{x}_m(t)$ received by the mth COLD pair at time t with $x_{1,m}(t)$ and $x_{2,m}(t)$ denoting the observed components from x-axis dipole and z-axis loop can be, respectively, expressed as

$$\begin{aligned}\mathbf{x}_m(t) &= \begin{bmatrix} x_{1,m}(t) \\ x_{2,m}(t) \end{bmatrix} \\ &= \sum_{k=1}^{K} a_m(\theta_k) \begin{bmatrix} -\cos\alpha_k \\ -\sin\alpha_k e^{i\beta_k} \end{bmatrix} s_k(t) + \mathbf{n}_m(t)\end{aligned} \tag{7}$$

where $\mathbf{n}_m(t) = [\begin{smallmatrix} n_{1,m}(t) \\ n_{2,m}(t) \end{smallmatrix}]$ is the noise vectors at the mth COLD pair with its x-component noise $n_{1,m}(t)$ and z-component $n_{2,m}(t)$, which is assumed as independent and identically distributed circularly symmetric Gaussian random variables with mean zero and variance σ_n^2. The traditional LV-MUSIC is based on the LV polar model in Eq. (7), which inevitably ignores the structural information contained in the output of the vector array.

3. THE PROPOSED ALGORITHM

In this section, two quaternion polar models are firstly introduced to construct the AQ model; then based on the AQ model, a multiple-dimension (MD) parameter decoupled MUSIC (named AQ-MUSIC) algorithm is proposed by utilizing the RARE principle for the DOAs.

Let $x_{1,m}(t)$ and $x_{2,m}(t)$ be the output of two sub-arrays constituted by dipoles and loops, which can be given by

$$\begin{aligned}x_{1,m}(t) &= \sum_{k=1}^{K} a_m(\theta_k)\xi_{k,1}s_k(t) + n_{1,m}(t) \\ x_{2,m}(t) &= \sum_{k=1}^{K} a_m(\theta_k)\xi_{k,2}s_k(t) + n_{2,m}(t)\end{aligned} \tag{8}$$

or in matrix form,

$$\begin{aligned}\mathbf{x}_1(t) &= \mathbf{Q}_1\mathbf{s}(t) + \mathbf{n}_1(t) \\ \mathbf{x}_2(t) &= \mathbf{Q}_2\mathbf{s}(t) + \mathbf{n}_2(t)\end{aligned} \tag{9}$$

where $\mathbf{Q}_l = [\mathbf{a}_1\xi_{1,l}, \ldots, \mathbf{a}_K\xi_{K,l}]$, $l = 1, 2$ is the angle-polarization array manifold matrices; $\mathbf{s}(t) = [s_1(t), \ldots, s_K(t)]^T$ is the signal vector; and $\mathbf{n}_l(t) = [n_{l,1}(t), \ldots, n_{l,M}(t)]^T$ is the noise vector of each sub-array.

Then, define $\mathbf{A} = [\mathbf{a}_1, \ldots, \mathbf{a}_K], \mathbf{V}_l = \mathrm{diag}\{\xi_{1,l}, \ldots, \xi_{K,l}\}$, and a quaternion-based array output vector can be constructed as follows

$$\mathbf{x}(t) = \mathbf{x}_1(t) + \mathbf{x}_2(t)j = \mathbf{A}\mathbf{V}_x\mathbf{s}(t) + \mathbf{n}_x(t) \tag{10}$$

where $\mathbf{V}_x = \mathbf{V}_1 + \mathbf{V}_2 j = \text{diag}\{\xi_{1,1} + \xi_{1,2}j, \ldots, \xi_{K,1} + \xi_{K,2}j\} \in \mathbb{H}^{K\times K}$, $\mathbf{n}_x(t) = \mathbf{n}_1(t) + \mathbf{n}_2(t)j \in \mathbb{H}^{M\times 1}$.

To proceed, another quaternion-based array output vector is defined as follows

$$\mathbf{y}(t) = \mathbf{x}_2(t) + \mathbf{x}_1(t)j = \mathbf{A}\mathbf{V}_y\mathbf{s}(t) + \mathbf{n}_y(t) \tag{11}$$

where $\mathbf{V}_y = \mathbf{V}_2 + \mathbf{V}_1 j = \text{diag}\{\xi_{1,2} + \xi_{1,1}j, \ldots, \xi_{K,2} + \xi_{K,1}j\} \in \mathbb{H}^{K\times K}$, $\mathbf{n}_y(t) = \mathbf{n}_2(t) + \mathbf{n}_1(t)j \in \mathbb{H}^{M\times 1}$.

Then, an AQ array output vector can be formed by concatenating $\mathbf{x}(t)$ and $\mathbf{y}(t)$,

$$\mathbf{z}(t) = \begin{bmatrix} \mathbf{x}(t) \\ \mathbf{y}(t) \end{bmatrix} = \begin{bmatrix} \mathbf{A}\mathbf{V}_x \\ \mathbf{A}\mathbf{V}_y \end{bmatrix} \mathbf{s}(t) + \begin{bmatrix} \mathbf{n}_x(t) \\ \mathbf{n}_y(t) \end{bmatrix}. \tag{12}$$

The AQ covariance matrix $\mathbf{R}$ of $\mathbf{z}(t)$ is calculated by

$$\begin{aligned} \mathbf{R} &= E\left\{\mathbf{z}(t)\mathbf{z}^H(t)\right\} \\ &= \begin{bmatrix} \mathbf{A}\mathbf{V}_x \\ \mathbf{A}\mathbf{V}_y \end{bmatrix} \mathbf{R}_s \begin{bmatrix} \mathbf{A}\mathbf{V}_x \\ \mathbf{A}\mathbf{V}_y \end{bmatrix}^H + 2\sigma_n^2\mathbf{I}_{2M} \\ &= \bar{\mathbf{A}}\mathbf{R}_s\bar{\mathbf{A}}^H + 2\sigma_n^2\mathbf{I}_{2M} \end{aligned} \tag{13}$$

where $\mathbf{R}_s{=}E\{\mathbf{s}(t)\mathbf{s}^H(t)\}$ is the signal covariance matrix, and $\bar{\mathbf{A}}$ is the extended array manifold matrix related to (θ, α, β). Obviously, $\mathbf{R}$ is a self-conjugated quaternion covariance matrix, and its complex adjoint matrix $\mathbf{R}^\sigma$ is a complex Hermite matrix. On the basis of the complex adjoint matrix defined in Eq. (3), we perform EVD on $\mathbf{R}^\sigma$ as follows

$$\begin{aligned} \mathbf{R}^\sigma &= \begin{pmatrix} \mathbf{R}_1 & \mathbf{R}_2 \\ -\mathbf{R}_2^* & \mathbf{R}_1^* \end{pmatrix} \\ &= \begin{pmatrix} \mathbf{U}_1 & \mathbf{U}_2 \\ -\mathbf{U}_2^* & \mathbf{U}_1^* \end{pmatrix} \begin{pmatrix} \mathbf{\Lambda} & \mathbf{0} \\ \mathbf{0} & \mathbf{\Lambda} \end{pmatrix} \begin{pmatrix} \mathbf{U}_1 & \mathbf{U}_2 \\ -\mathbf{U}_2^* & \mathbf{U}_1^* \end{pmatrix}^H. \end{aligned} \tag{14}$$

The EVD of $\mathbf{R}$ has the form of

$$\begin{aligned} \mathbf{R} &= \mathbf{U}\mathbf{\Lambda}\mathbf{U}^H \\ &= (\mathbf{U}_1 + \mathbf{U}_2 j)\mathbf{\Lambda}(\mathbf{U}_1 + \mathbf{U}_2 j)^H \\ &= \mathbf{U}_s\mathbf{\Lambda}_s\mathbf{U}_s^H + \mathbf{U}_n\mathbf{\Lambda}_n\mathbf{U}_n^H \end{aligned} \tag{15}$$

where $\mathbf{U}_s \in \mathbb{H}^{2M\times K}$ is the quaternion-based signal subspace corresponding to eigenvalue matrices $\mathbf{\Lambda}_s$, and $\mathbf{U}_n \in \mathbb{H}^{2M\times(2M-K)}$ is the quaternion-based noise subspace corresponding to eigenvalue matrices $\mathbf{\Lambda}_n$.

Similar to the orthogonality relationship in complex-valued MUSIC method [5], the quaternion matrix $\mathbf{U}_s$ is still orthogonal to $\mathbf{U}_n$. Furthermore, the extended array manifold matrix $\bar{\mathbf{A}}$ and signal subspace $\mathbf{U}_s$ span the same subspace [5], thus $\bar{\mathbf{A}}$ is also orthogonal to $\mathbf{U}_n$, namely,

$$\bar{\mathbf{a}}^H\mathbf{U}_n = \mathbf{0} \tag{16}$$

where $\bar{\mathbf{a}}$ is the column vector of $\bar{\mathbf{A}}$. Based on Eq. (16), the spectrum function of AQ-MUSIC is constructed as

$$f_Q(\theta, \alpha, \beta) = \left\|\bar{\mathbf{a}}^H(\theta, \alpha, \beta)\mathbf{U}_n\right\|_F^2 \tag{17}$$

where

$$\begin{aligned} \bar{\mathbf{a}}(\theta) &= \begin{bmatrix} \mathbf{a}(\theta)(\xi_{k,1} + \xi_{k,2}j) \\ \mathbf{a}(\theta)(\xi_{k,2} + \xi_{k,1}j) \end{bmatrix} \\ &= \dot{\mathbf{a}}(\theta) \begin{bmatrix} \xi_{k,1} + \xi_{k,2}j \\ \xi_{k,2} + \xi_{k,1}j \end{bmatrix} \end{aligned} \tag{18}$$

where $\dot{\mathbf{a}}(\theta) = \text{blkdiag}\{\mathbf{a}(\theta), \mathbf{a}(\theta)\}$. Substituting Eq. (18) to Eq. (17), the spectrum function $f_Q(\theta, \alpha, \beta)$ can be changed to

$$\begin{aligned} f_Q(\theta, \alpha, \beta) &= \begin{bmatrix} \xi_{k,1} + \xi_{k,2}j \\ \xi_{k,2} + \xi_{k,1}j \end{bmatrix}^H \dot{\mathbf{a}}^H(\theta)\,\mathbf{U}_n\mathbf{U}_n^H\dot{\mathbf{a}}(\theta) \begin{bmatrix} \xi_{k,1} + \xi_{k,2}j \\ \xi_{k,2} + \xi_{k,1}j \end{bmatrix} \\ &= \boldsymbol{\varepsilon}^H(\alpha, \beta)\mathbf{C}(\theta)\,\boldsymbol{\varepsilon}(\alpha, \beta) \end{aligned} \tag{19}$$

where

$$\mathbf{C}(\theta) = \dot{\mathbf{a}}^H(\theta)\mathbf{U}_n\mathbf{U}_n^H\dot{\mathbf{a}}(\theta), \boldsymbol{\varepsilon}(\alpha, \beta) = \begin{bmatrix} \xi_{k,1} + \xi_{k,2}j \\ \xi_{k,2} + \xi_{k,1}j \end{bmatrix} \tag{20}$$

As $0 \leq \alpha_k \leq \pi/2$, $\xi_{k,1} + \xi_{k,2}j$ and $\xi_{k,2} + \xi_{k,1}j$ are not equal to zero in general, thus $\boldsymbol{\varepsilon}(\alpha, \beta) \neq 0$. In general, the matrix $\mathbf{C}(\theta)$ is full rank with the assumption of $K \leq M$. However, when the true DOA presents, which is $\theta = \theta_k, k = 1, \ldots K$, the matrix $\mathbf{C}(\theta)$ is rank deficient or equivalently $\det[\mathbf{C}(\theta)] = 0$. Based on the RARE principle [13, 14], the spectrum function $f_Q(\theta, \alpha, \beta)$ can be simplified as

$$f_Q(\theta) = \frac{1}{\det[\mathbf{C}(\theta)]} \tag{21}$$

By searching over $\theta \in [-\frac{\pi}{2}, \frac{\pi}{2}]$, the DOA estimates of all sources can be obtained from the K highest peaks. A flowchart of the proposed algorithm is shown in Fig. 1.

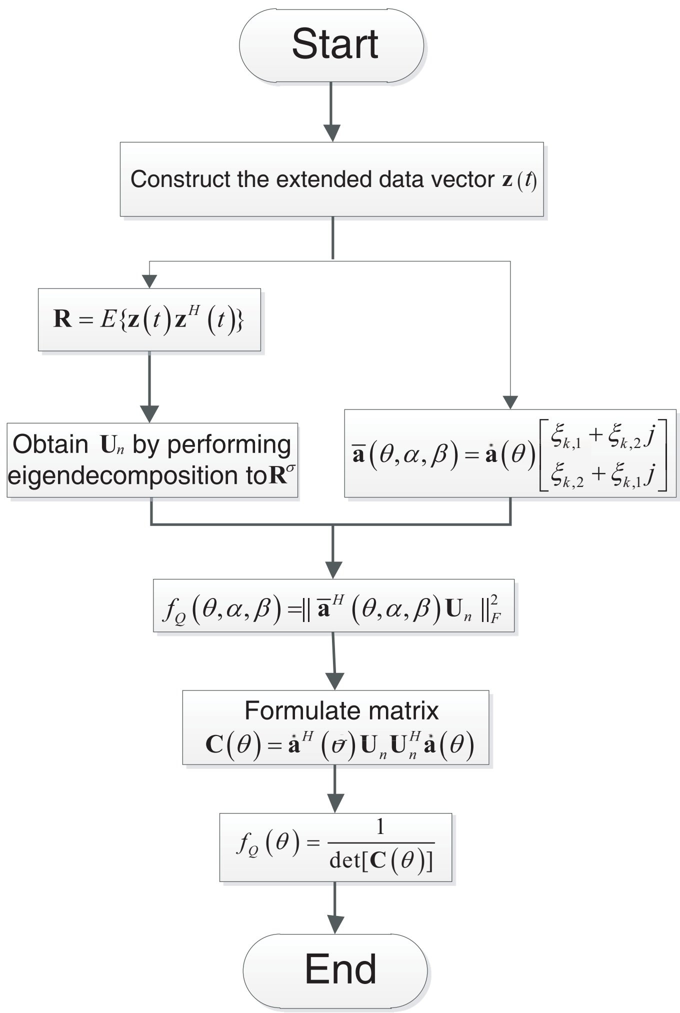

Figure 1. The flowchart of the proposed algorithm.

4. SIMULATION RESULTS

Several examples are conducted in this section, to verify the performance of the proposed AQ-MUSIC algorithm, as compared to LV-MUSIC [5] and Q-MUSIC [9]. Consider a ULA of COLDs with half-wavelength inter-element spacing, illuminated by three uncorrelated equal-power signals, which have the interesting parameters $(\theta_1, \alpha_1, \beta_1) = (10°, 22°, 35°)$, $(\theta_2, \alpha_2, \beta_2) = (30°, 33°, 45°)$ and $(\theta_3, \alpha_3, \beta_3) = (45°, 44°, 60°)$, respectively. The noise of the COLD element which is additive white Gaussian with zero-mean is uncorrelated with the incoming signals. The root mean squared error (RMSE), calculated by 500 Monte Carlo trials, is adopted as the performance index.

In the first example, the DOA estimation performance is studied with respect to SNR. The number of elements is 8, and the SNR varies from -6 dB to 18 dB. The number of snapshots T adopted is 50. Fig. 2 shows that the AQ-MUSIC algorithm has clearly outperformed the Q-MUSIC and LV-MUSIC algorithms, especially in low SNR regions.

In the second example, the average received SNR of each signal is 5 dB. The RMSEs of the estimated DOA parameter versus the number of snapshots are depicted in Fig. 3. As shown in Fig. 3, the RMSEs of the estimated DOAs of all three algorithms decrease as the number of snapshots increases. From the results, the AQ-MUSIC provides more accurate DOA estimation than other counterparts with a small

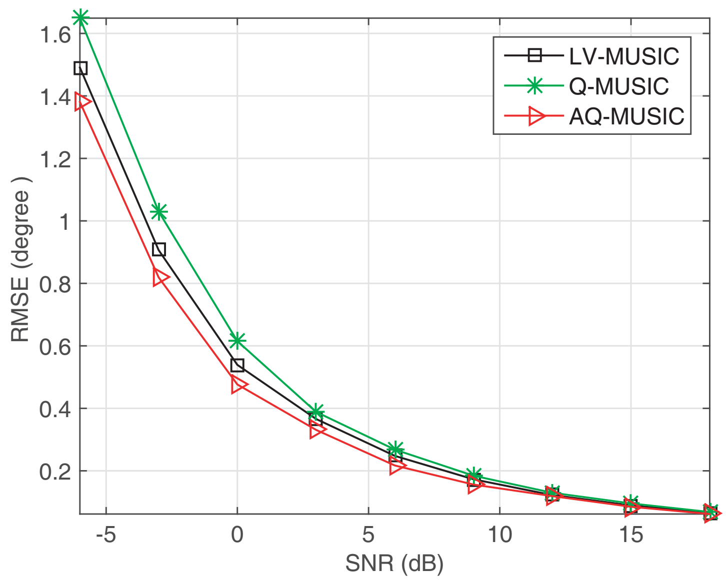

Figure 2. RMSE versus SNR.

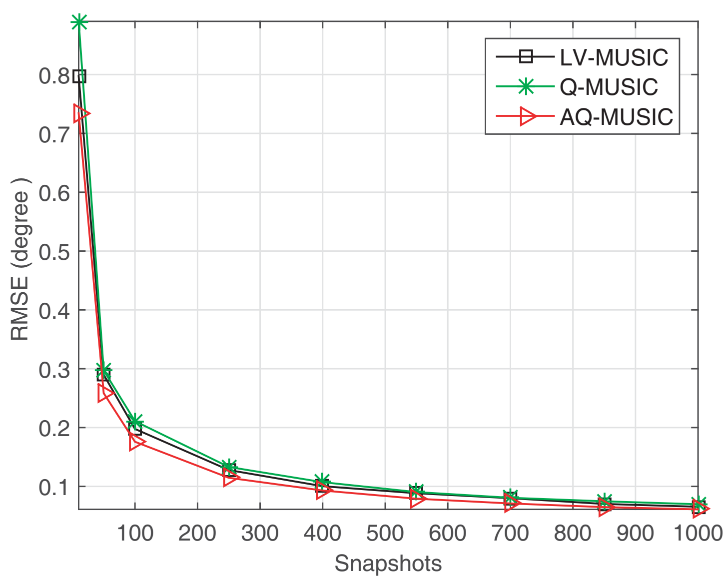

Figure 3. RMSE versus snapshots.

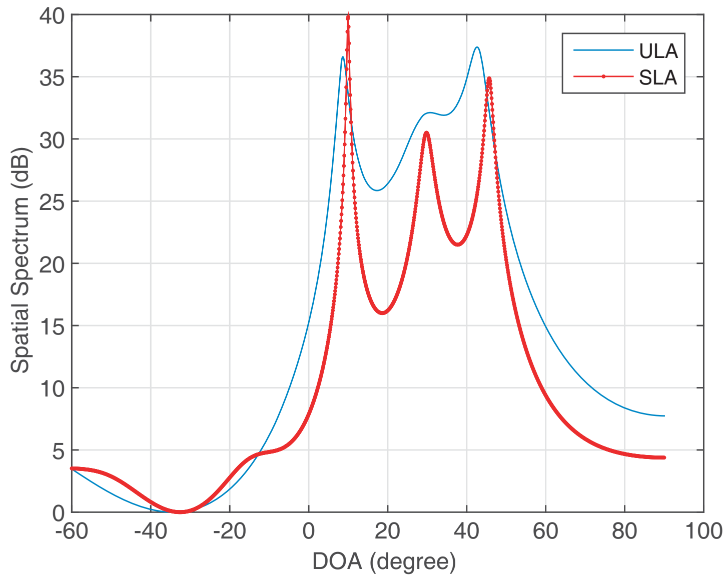

Figure 4. Spatial resolution capability.

number of snapshots.

In the third example, the spatial resolution capability of the AQ-MUSIC method is demonstrated based on a ULA/SLA of 4 elements with SNR = 20 dB and 10 snapshots. Fig. 4 shows that the AQ-MUSIC algorithm based on SLA has clearly distinguished the DOAs with sharper peaks than ULA.

5. CONCLUSION

By utilizing a COLD array, an AQ-MUSIC algorithm is proposed for DOA estimation of fully polarized signals. With judiciously arranging the observed signals, an AQ data model is constructed, and the AQ noise subspace is achieved by performing EVD on the adjoint matrix of AQ covariance matrix. Based on the orthogonality relationship, the AQ-MUSIC estimator is built to achieve the DOAs corresponding to the peaks. In comparison with the existing MUSIC-type counterparts, the proposed AQ-MUSIC method yields an overall improved performance in low SNRs with small number of snapshots.

ACKNOWLEDGMENT

This work was supported by the National Natural Science Foundation of China under Grant 62001256, and by Key Laboratory of Intelligent Perception and Advanced Control of State Ethnic Affairs Commission under Grant MD-IPAC-2019102, and by Zhejiang Provincial Natural Science Foundation of China under Grant LQ19F010002, and by the Scientific Research Foundation of Graduate School of Ningbo University under Grant IF2020112, and by Zhejiang Xin Miao Talent Plan under Grant 2020R405029, and by K. C. Wong Magna Fund in Ningbo University.

REFERENCES

1. Chintagunta, S. and P. Ponnusamy, "Spatial and polarization angle estimation of mixed-targets in MIMO radar," *Progress In Electromagnetics Research M*, Vol. 82, 49–59, 2019.
2. Shu, T., J. He, X. Han, X. Li, and K. Yu, "Joint DOA and degree-of-polarization estimation of partially-polarized signals using nested arrays," *IEEE Communications Letters*, Vol. 24, No. 10, 2182–2186, 2020.

3. Chen, H., W. Wang, and W. Liu, "Joint DOA, range, and polarization estimation for rectilinear sources with a COLD array," *IEEE Wireless Communications Letters*, Vol. 8, No. 5, 1398–1401, Oct. 2019.
4. Wang, W., H. Chen, J. Jin, X. Wang, L. Wan, and X. Zhang, "Quaternion-MUSIC for near-field strictly noncircular sources with large-scale polarization array," *Digital Signal Processing*, Vol. 94, 137–145, Nov. 2019.
5. Nehorai, A. and E. Paldi, "Vector-sensor array processing for electromagnetic source localization,"*IEEE Transactions on Signal Processing*, Vol. 42, No. 2, 376–398, Feb. 1994.
6. Yue, Y., Y. Xu, Z. Liu, and L. Shen, "Parameter estimation of coexisted circular and strictly noncircular sources using diversely polarized antennas," *IEEE Communications Letters*, Vol. 22, No. 9, 1822–1825, 2018.
7. Li, J. and R. T. Compton, "Angle and polarization estimation using ESPRIT with a polarization sensitive array," *IEEE Transactions on Antennas and Propagation*, Vol. 39, No. 9, 1376–1383, Sept. 1991.
8. Zoltowski, M. D. and K. T. Wong, "ESPRIT-based 2-D direction finding with a sparse array of electromagnetic vector-sensors," *IEEE Transactions on Signal Processing*, Vol. 48, No. 8, 2195–2204, Aug. 2000.
9. Miron, S., N. Le Bihan, and J. I. Mars, "Quaternion-MUSIC for vector-sensor array processing," *IEEE Transactions on Signal Processing*, Vol. 54, No. 4, 1218–1229, Apr. 2006.
10. Le Bihan, N., S. Miron, and J. I. Mars, "MUSIC algorithm for vector-sensors array using biquaternions," *IEEE Transactions on Signal Processing*, Vol. 55, No. 9, 4523–4533, Sept. 2007.
11. Gong, X., Z. Liu, and Y. Xu, "Quad-quaternion MUSIC for DOA estimation using electromagnetic vector sensors," *EURASIP Journal on Advances in Signal Processing*, Vol. 2008, 204, 2008.
12. Castorina, G., L. Di Donato, A. F. Morabito, T. Isernia, and G. Sorbello, "Analysis and design of a concrete embedded antenna for wireless monitoring applications," *IEEE Antennas and Propagation Magazine*, Vol. 58, No. 6, 76–93, Dec. 2016.
13. Chen, H., W. Liu, W. Zhu, M. Swamy, and Q. Wang, "Mixed rectilinear sources localization under unknown mutual coupling," *Journal of the Franklin Institute*, Vol. 356, No. 4, 2372–2394, 2019.
14. Chen, H., W.-P. Zhu, W. Liu, et al., "RARE-based localization for mixed near-field and far-field rectilinear sources," *Digit. Signal Process.*, Vol. 85, 54–61, Feb. 2019.